SIMULATED LOW-GRAVITY SLOSHING IN CYLINDRICAL TANKS INCLUDING EFFECTS OF DAMPING AND SMALL LIQUID DEPTH

by

Franklin T. Dodge
Luis R. Garza

Technical Report No. 5
Contract NAS8-20290
Control No. DCN 1-6-75-00010
SwRI Project No. 02-1846

Prepared for

George C. Marshall Space Flight Center
National Aeronautics and Space Administration
Huntsville, Alabama

29 December 1967

SOUTHWEST RESEARCH INSTITUTE
SAN ANTONIO HOUSTON

SOUTHWEST RESEARCH INSTITUTE
8500 Culebra Road, San Antonio, Texas 78228

Department of Mechanical Sciences

SIMULATED LOW-GRAVITY SLOSHING IN CYLINDRICAL TANKS INCLUDING EFFECTS OF DAMPING AND SMALL LIQUID DEPTH

by

Franklin T. Dodge
Luis R. Garza

Technical Report No. 5
Contract NAS8-20290
Control No. DCN 1-6-75-00010
SwRI Project No. 02-1846

Prepared for

George C. Marshall Space Flight Center
National Aeronautics and Space Administration
Huntsville, Alabama

29 December 1967

APPROVED:

H. Norman Abramson

H. Norman Abramson, Director
Department of Mechanical Sciences

FOREWORD

This report is the third in a series of Technical Reports concerned with fuel sloshing under low-gravity conditions. Reference to the first two reports ("Experimental and Theoretical Studies of Liquid Sloshing at Simulated Low Gravities," TR No. 2, Contract NAS8-20290, 20 October 1966, and "Low Gravity Liquid Sloshing in an Arbitrary Axisymmetric Tank Performing Translational Oscillations," TR No. 4, Contract NAS8-20290, 20 March 1967) will aia in understanding some of the experimental procedures and theoretical analyses that are presented in abbreviated form in the present report.

ABSTRACT

Liquid sloshing in cylindrical tanks is studied under conditions of simulated low gravities. The effects of finite liquid depths and the determination of the smooth wall damping are emphasized. The experimental and theoretical results show that the fluid dynamics are affected by small h/d ratios in much the same way as for normal, large Bond number sloshing. Measurements of the slosh damping indicate that the damping increases as the Bond number decreases, and two correlation equations for the damping factor are proposed. An equivalent mechanical model developed previously is extended to include h/d variations and linear viscous damping. Comparisons of the force response predicted by the model to that measured in the tests verify the model to a high degree of confidence.

TABLE OF CONTENTS

		Page
LIST OF ILLUSTRATIONS		v
LIST OF PRINCIPAL SYMBOLS		vi
I.	INTRODUCTION	1
II.	EXPERIMENTAL APPARATUS AND PROCEDURE	2
III.	TEST RESULTS	3
	A. Force Response	3
	B. Slosh Damping	4
IV.	COMPARISON OF THEORY AND EXPERIMENT	10
V.	CONCLUSIONS	12
VI.	LIST OF REFERENCES	13
APPENDIXES		15
	A. Theory-Mechanical Model	15
	B. Illustrations	16

LIST OF ILLUSTRATIONS

Figure		Page
1	Dynamometer Package on Shake Table	17
2	Response Curves for CCl_4 in 1.36" Dia. Tank, $N_{BO} = 175$	18
3	Response Curves for Methanol in 1.36" Dia. Tank, $N_{BO} = 100$	19
4	Response Curves for CCl_4 in 1.04" Dia. Tank, $N_{BO} = 100$	20
5	Response Curves for Methanol in 1.04" Dia. Tank, $N_{BO} = 60$	21
6	Response Curves for CCl_4 in 0.688" Dia. Tank, $N_{BO} = 45$	22
7	Response Curves for Methanol in 0.688" Dia. Tank, $N_{BO} = 26$	23
8	Response Curves for CCl_4 in 0.383" Dia. Tank, $N_{BO} = 14$	24
9	Variation of Smooth Wall Damping Coefficient with Galileo Number	25
10	Variation of γ_s with Correlation Equation of Clark and Stephens [6]	26
11	Variation of Incremental Damping Factor with Bond Number	27
12	Variation of Slosh Natural Frequency with Bond Number	28
13	Variation of Slosh Mass with Bond Number	29
14	Variation of Spring Constant with Bond Number	30
15	Comparison of Theoretical and Experimental Force-Response Curves	31

LIST OF PRINCIPAL SYMBOLS

Symbol

d	-	diameter of tank
f	-	frequency of tank excitation
f_1	-	natural frequency or resonant frequency of sloshing
g	-	acceleration of gravity or equivalent linear acceleration
h	-	depth of liquid below bottom of meniscus
m_1	-	slosh mass in mechanical model
k_1	-	spring constant in mechanical model
m_o	-	rigidly attached mass in mechanical model
m_T	-	$m_o + m_1$, total liquid mass
N_{BO}	-	Bond number
N_{GA}	-	Galileo number
R_o	-	tank radius
x_o	-	amplitude of tank excitation
γ_s	-	slosh damping coefficient
δ	-	amplitude of slosh wave
ν	-	kinematic viscosity

I. INTRODUCTION

The sloshing of the liquid fuel contained in a space system can strongly affect the performance of the system. During launch and powered flight, the liquid fuel is acted upon by strong body forces, but, during orbital coasting or in deep space, the body forces or "gravity" forces are reduced substantially, and the liquid motion is governed by other, primarily surface, forces. Sloshing under these conditions is usually called "low-g" sloshing or, more exactly, "low Bond number" sloshing.

Because of the lack of a convenient low gravity laboratory, not much data exist concerning low-g sloshing. Habip [1]* has reviewed most of the pertinent work done prior to 1965, and, recently, Yeh [2] and Chu [3] have studied analytically low-g sloshing in axisymmetric tanks; however, no numerical examples were given. As part of a study of the Apollo spacecraft propulsion system, a number of approximate analyses of low-g liquid motions, such as reorientation, ullage gas entrainment, and sloshing have been formulated [4], but these analyses pertain to nearly zero gravity, a regime where almost no experimental data are available for verification of the analyses. In Technical Report No. 2 of the present contract [5], a theoretical and experimental study of moderately low-g sloshing in cylindrical tanks was given. The experimental results were obtained by simulating low gravity (actually, small Bond numbers) through the use of small tanks. Clark and Stephens [6] also obtained data on low-g slosh damping and natural frequency by this same method. Other experimental results have been gathered by free-fall tests in "drop towers" [7,8]. All of these results, in general, are for specialized tank geometries or situations, and no theory has yet been able to explain completely the dynamics of low-g sloshing throughout the range from true zero-gravity (zero Bond number) to normal or high gravity (large Bond numbers).

The purpose of the work reported here was to extend the research described in Ref. [5] to include the effects of small liquid height-to-tank diameter ratios and to determine the magnitude of viscous damping under small Bond number conditions. Three different liquids (carbon tetrachloride, methanol, and acetone) were tested in four different tanks (diameters: 1.36 in., 1.04 in., 0.688 in., and 0.383 in.); this was sufficient to cover the range of Bond numbers from 14 to 175.

---

*Numbers in brackets denote references listed in Section VI of this report.

II. EXPERIMENTAL APPARATUS AND PROCEDURE

With two major exceptions, the experimental setup used in the present tests was similar to that described in Ref. [5]. First, instead of attaching the small dynamometer package directly to the armature of SwRI's 1100-lb electromagnetic shaker, the experimental package was attached to a massive horizontal shake table which was then excited in pure translation by a much smaller, 50-lb output electromagnetic shaker. The dynamometer package (without its protective cover) is shown attached to the shake table in Fig. 1; the tank on the left, with an inverted ellipsoidal bottom, is one used in other tests. Because of the linear ball bearings guiding the shake table and the general ruggedness of the supports, an excellent sinusoidal excitation signal, with little out-of-plane motion, was obtained.* This improvement, and an improvement in the electronic amplification system of the slosh force signal, allowed sufficiently small excitation amplitudes to be used to sweep completely through the slosh resonance frequency without encountering swirling motion of the liquid. Thus, slosh damping factors could be obtained by the usual half-bandwidth technique. Second, a carbon film potentiometer was attached directly to the support frame; this allowed a continuous monitoring of the displacement amplitude with a consequent large improvement in the accuracy of the data.

The experimental procedures, calibrations, and data reductions were the same as reported previously [5]. Briefly, however, two tanks are used for each test; one tank, empty, and called the balance tank, is used to cancel the inertia of the other tank, containing the test liquid and called the active tank, so that the residual force felt by the dynamometer when the active tank is empty is very small. The sloshing force is detected by semiconductor strain gages (gage factor = 118) mounted on the tension-compression arms of the dynamometer; the output of the gages is amplified and recorded on an oscillograph. The excitation frequency, which could be maintained to the fourth significant figure of the period (in seconds), is determined with a digital period counter.

*The shake table is described in Ref. [9].

III. TEST RESULTS

There were two main objectives of the experimental program: (1) measure the lateral slosh force for the fundamental mode as a function of the excitation frequency and amplitude, and (2) measure the slosh damping present. The parameters to be varied were the Bond number and the liquid depth.

All of the tests were run with glass tanks and reagent grade liquids. As nearly as could be determined visually, the contact angle was zero degrees for all the liquids against the tank walls, and the sloshing motion of the liquids appeared to approximate the "free edge" or no contact angle hysteresis condition very well.

A. Force Response

Figures 2 through 8 show typical force response curves for CCl_4 and methanol. (The force response of acetone in every case was nearly identical to that of methanol, except for the peak force at resonance, which depends on the magnitude of the slosh damping present; thus, the results for acetone are not shown, although the damping factor was computed and will be discussed later.) The solid lines in these figures are faired curves through the experimental data. To facilitate direct comparisons, neither the force nor the frequency is nondimensionalized in any way. Note that the combination of small excitation amplitudes, very little out-of-plane motion of the shake table, and the natural slosh damping allowed complete resonance curves to be obtained; that is, no liquid swirling or rotation was evident.

The range of Bond numbers covered by the figures is from 175 (CCl_4 in 1.36-in. diameter tank) to 14 (CCl_4 in 0.383-in. diameter tank) with liquid depth-to-tank diameter ratios (h/d) from 0.25 to 1.25. Even larger h/d ratios were used in some tests, but these results were substantially the same as for h/d = 1.00 or 1.25.* Other information given in the figures includes the amplitude of tank excitation (x_0), the resonant frequency (f_1) as determined by the peak in the response curve, the slosh damping coefficient (γ_s) as determined by the half-bandwidth technique, and the wave height (δ) at resonance.

By comparing the resonant frequency, f_1, to that calculated by theoretical results for the undamped natural frequency at large Bond

*The depth of liquid below the bottom of the curved meniscus is used in computing h/d. The average liquid depth is larger than h by an amount 0.132 βd where β is the root of $\beta^3 N_{BO} - \beta^2 - 2/3 = 0$ [5].

numbers [i.e., $2\pi f_1 = \left\{3.682\ (g/d) \tanh 3.682\ (h/d)\right\}^{1/2}$], it can be seen that the resonant frequency for N_{BO} = 175 is slightly lower than the corresponding high-g frequency for the same h and d. As the Bond number is decreased, however, the resonant frequency increases rapidly above the high-g frequency. This is similar to the results, presented in Ref. [5], which have been confirmed by Clark and Stephens [6]. Furthermore, the decrease in f_1 as h/d is decreased is less for small N_{BO}'s. Comparisons of theory and experiment made in the next section of the report verify these observations.

Some slight nonlinearity is evident in the force-response curves, especially for the smaller h/d ratios or for the larger γ_s's. Qualitatively, however, the force response even for the smallest N_{BO} of 14 is similar to ordinary large Bond number sloshing.

B. Slosh Damping

For each resonant force response curve, the equivalent viscous damping present in the sloshing was computed by the half-bandwidth technique. The resulting damping coefficient, γ_s, is given on the next page in Table I as a function of h/d and N_{BO}. (γ_s is defined as the ratio of the apparent damping to the critical damping and is equivalent to the logarithmic decrement divided by 2π.)

All of the damping data for $h/d \geq 1.0$ are shown graphically in Fig. 9. (For smaller h/d, γ_s varies with the liquid depth, but no change in damping was apparent for $h/d \geq 1.0$; this agrees with high Bond number results.) The abscissa in Fig. 9 is $N_{GA}^{-1/2}$, N_{GA} being the Galileo number, a form of the Reynolds number pertinent to high Bond number sloshing. Although N_{GA} is usually defined as $g^{1/2}R_o^{3/2}\nu^{-1}$, it is clear on both dimensional and theoretical grounds that "g" really enters by way of the natural frequency [i.e., $f_1 \propto (g/R_o)^{1/2}$ when $N_{BO} = \infty$]. Thus, for small N_{BO}'s, $N_{GA}^{-1/2}$ should be defined as $0.465\ \nu^{1/2} f_1^{-1/2} R_o^{-1}$ in order to eliminate g since here f_1 is not directly proportional to $(g/R_o)^{1/2}$; the factor 0.465 is necessary to insure that this definition of $N_{GA}^{-1/2}$ and the usual one are the same for large N_{BO}'s.*

Both experiment [10] and theory [11] have shown that γ_s is directly proportional to $N_{GA}^{-1/2}$ for large Bond number conditions. The data included in Fig. 9 also show this since a large N_{BO} corresponds to a small N_{GA} on this plot. But, for small N_{BO} (large $N_{GA}^{-1/2}$), γ_s is considerably larger than that predicted by the usual correlation equation $\gamma_s = 0.83\ N_{GA}^{-1/2}$, which is valid for large N_{BO}'s. Other experimenters have also observed the increase in γ_s [6, 12]. On a purely empirical basis, Keulegan [12] and Clark and Stephens [6] concluded that γ_s should be calculated as the sum of two parts:

*That is, $0.465\ \nu^{1/2} f_1^{-1/2} R_o^{-1} = \nu^{1/2} g^{-1/4} R_o^{-3/4}$ when $2\pi f_1 = [1.841\ (g/R_o)]^{1/2}$.

TABLE I

SUMMARY OF DAMPING DATA

Tank Diameter (in.)	Liquid	h/d	x_o(in.)	γ_s	$N_{BO} = \rho g R_o^2/T$	$N_{Ga}^{-\frac{1}{2}} = .46\nu^{\frac{1}{2}} f_1^{-\frac{1}{2}} R_o^{-1}$
1.36	CCl_4	1.250	0.0015	0.011	175	0.0089
			0.002	0.009		
		0.750	0.0015	0.009		
			0.002	0.010		
		0.500	0.002	0.010		
		0.375	0.002	0.010		
			0.003	0.008		
		0.250	0.002	0.009		
			0.003	0.009		
1.36	Acetone	1.250	0.0015	0.009	95	0.0074
1.36	Methanol	1.250	0.002	0.013	100	0.0099
			0.003	0.014		
		0.750	0.002	0.012		
			0.003	0.013		
		0.500	0.002	0.015		
			0.003	0.012		
		0.375	0.002	0.014		
			0.003	0.016		
		0.250	0.002	0.015		
			0.003	0.015		
			0.0045	0.017		
1.04	CCl_4	1.750	0.0015	0.016	100	0.0109
		1.500	0.0015	0.016		
		1.250	0.0015	0.016		
		1.000	0.0015	0.017		
		0.500	0.002	0.016		
		0.375	0.002	0.017		
			0.003	0.018		
		0.250	0.002	0.015		
			0.003	0.017		
1.04	Acetone	1.250	0.002	0.0095	55	0.009
1.04	Methanol	1.750	0.002	0.020	60	0.0121
		1.500	0.002	0.019		
		1.250	0.002	0.017		
		1.000	0.002	0.019		
			0.003	0.020		

TABLE I. SUMMARY OF DAMPING DATA (Cont'd)

Tank Diameter (in.)	Liquid	h/d	x_o(in.)	γ_s	$N_{BO} = \rho g R_o^2/T$	$N_{Ga}^{-\frac{1}{2}} = .46\nu^{\frac{1}{2}} f_1^{-\frac{1}{2}} R_o^{-1}$
1.04	Methanol (cont.)	0.75	0.002	0.018	60	0.0121
			0.003	0.023		
		0.50	0.002	0.018		
		0.375	0.002	0.019		
			0.003	0.021		
		0.250	0.003	0.019		
			0.004	0.020		
0.688	CCl_4	1.750	0.004	0.027	45	0.0149
		1.25	0.002	0.021		
			0.003	0.021		
			0.004	0.017		
		0.750	0.002	0.024		
			0.003	0.023		
			0.004	0.021		
		0.500	0.002	0.023		
			0.003	0.023		
			0.004	0.022		
		0.250	0.002	0.038		
			0.003	0.029		
			0.004	0.032		
0.688	Acetone	1.250	0.003	0.0165	25	0.0124
0.688	Methanol	1.250	0.002	0.022	26	0.0165
			0.003	0.026		
			0.004	0.026		
		0.750	0.002	0.026		
			0.003	0.027		
			0.004	0.026		
		0.500	0.002	0.029		
			0.003	0.025		
			0.004	0.027		
		0.250	0.002	0.029		
			0.003	0.046?		
			0.004	0.037?		
0.383	CCl_4	1.750	0.003	0.052	14	0.023
			0.004	0.047		
		1.500	0.003	0.045		
			0.004	0.042		
		1.25	0.003	0.044		
			0.004	0.035		
		1.000	0.003	0.055		
			0.004	0.049		
		0.750	0.003	0.042		
			0.004	0.044		
		0.500	0.003	0.039		
			0.004	0.032		
		0.375	0.004	0.042		
			0.005	0.039		

$$\gamma_s = \gamma_{N_{GA}} + \gamma_{N_{BO}} \tag{1}$$

where $\gamma_{N_{GA}}$ is a function only of the Galileo number and $\gamma_{N_{BO}}$ only of the Bond number; furthermore, $\gamma_{N_{BO}} \rightarrow 0$ as $N_{BO} \rightarrow \infty$. Clark and Stephens [6] were able to correlate their data (which are the ○ and □ points in Fig. 9) in this way by using the equation

$$\gamma_s = 0.83\ N_{GA}^{-1/2} + 0.096\ N_{BO}^{-3/5} \tag{2}$$

which reduces to the correct relation as $N_{BO} \rightarrow \infty$ but predicts that $\gamma_s \rightarrow \infty$ as $N_{BO} \rightarrow 0$. In the range tested by them ($8 < N_{BO} < 1000$), Eq. (2) gave a very close fit to their data, although Keulegan in his work with rectangular tanks [11] found that $\gamma_{N_{BO}}$ should vary as N_{BO}^{-1}. To check Eq. (2), the present data were tested against it, as shown in Fig. 10. The correlation is fairly good although not so good as the same equation with Clark and Stephens' original data. Part of the discrepancy may arise from the fact that the damping in Ref. [6] was based on the log decrement of the free decay of the sloshing wave, while the present damping results were based on forced response measurements; free decay tests and forced response tests are equivalent for linear systems, but this may not be true for slightly nonlinear systems such as these.

Neither Keulegan [12] nor Clark and Stephens [5] attempted an explanation of the physics behind the evident variation of γ_s with N_{BO}; in fact, it is not apparent why γ_s should vary independently with N_{BO} since no energy dissipation is provided by surface tension forces alone. J.W. Miles [13] has, however, analyzed the damping of surface waves in tanks by using various approximations to the dissipation provided by viscosity, by diffusion from the bulk liquid to the surface and vice versa during the stretching and contracting of the free surface when it oscillates, by soluble or insoluble films or contaminants on the free surface, and by contact angle hysteresis. He proposed that γ_s should be calculated as

$$\gamma_s = \gamma_{N_{GA}}(1 + \gamma_s') + \gamma_L \tag{3}$$

γ_s' is a parameter dependent upon surface properties; for insoluble surface films (in which the variation of the surface tension as the surface stretches is proportional to the undisturbed surface tension), γ_s' depends only on a parameter ξ:

$$\gamma_s' = \frac{\xi^2}{(\xi - 1)^2} \tag{4}$$

where

$$\xi \propto \frac{1}{N_{GA}}\left(\frac{gR_o}{f_1^2 N_{BO}}\right) \tag{5}$$

The third term, γ_L, is the contribution to the damping by contact angle hysteresis. According to Miles, both the advance and recession of the meniscus are opposed by constant forces that depend only on the material properties of the liquid-gas-tank interface. He showed that

$$\gamma_L = \frac{\kappa f(N_{BO})}{\delta} \tag{6}$$

where $f(N_{BO})$ depends only on N_{BO}, κ is the magnitude of the constant opposing force, and δ is the wave amplitude. For the present tests, γ_L should be very small (i.e., $\kappa \approx 0$) since no contact angle hysteresis was observed; furthermore, the data of Ref. [6] indicate no variation of γ_s with δ although some variation is evident in our results. For these reasons, a correlation of the form

$$\gamma_s = 0.83\ N_{GA}^{-1/2}\ (1 + AN_{BO}^n) \tag{7}$$

was attempted, which is in qualitative agreement with Miles' predicted form for the damping when γ_L is neglected. Results are shown in Fig. 11 in terms of the excess of the experimental γ_s over the expected high-g γ_s of $0.83\ N_{GA}^{-1/2}$, divided by the high-gγ_s; this quantity, called the incremental damping,

$$\frac{\gamma_s - 0.83\ N_{GA}^{-1/2}}{0.83\ N_{GA}^{-1/2}}$$

should depend only on N_{BO} according to Eq. (7). The best fit of the data to Eq. (7) was obtained with $A = 0.63$ and $n = -1/2$; the proposed correlation equation is then

$$\gamma_s = 0.83\ N_{GA}^{-1/2}\ (1 + 0.63\ N_{BO}^{-1/2}) \tag{8}$$

which gives a reasonably good correlation to both the present data and the data of Ref. [6].

Equation (8) has the merit that it shows that the energy dissipation arises through the viscosity; however, neither Eqs. (8) nor (2) can be correct for $N_{BO} = 0$. For $N_{BO} = 0$, the experimental results obtained by

Salzman et al. [7] using a drop tower indicate that $\gamma_s = 3.84\ N_{GA}^{-1/2}$; such a value of γ_s is predicted by Eq. (8) for $N_{BO} = 0.03$, and, thus, $N_{BO} = 0.03$ seems to be the absolute lower limit on the applicability of Eq. (8). Because of the form of Eq. (2), it cannot be compared directly to the data of Ref. [7], but, for $N_{BO} = 0.03$, Eq. (2) predicts that $\gamma_s = 0.83\ N_{GA}^{-1/2} + 0.78$, which is perhaps numerically larger than ought to be expected.

For h/d < 1.0, the trend of the damping data (Table I) is an increase in γ_s as h/d decreases. This is similar to the variation obtained for large Bond numbers, namely:

$$\gamma_s = 0.83\ N_{GA}^{-1/2} \tanh 1.84 \frac{h}{R_o} \left[1 + 2\left(1 - \frac{h}{R_o}\right) \operatorname{csch} 3.68 \frac{h}{R_o}\right]$$

However, for the smallest N_{BO} of 14, γ_s appears to decrease slightly as h/d decreases. For this reason, and because the amount of data collected is not sufficient to predict with any confidence the variation of γ_s with both h/d and N_{BO}, a correlation equation involving h/d has not been attempted.

IV. COMPARISON OF THEORY AND EXPERIMENT

For normal and high-g conditions, an equivalent mechanical model composed of masses, springs, and dashpots gives a very good representation of the force response characteristics of sloshing. Further, it was shown in Ref. [5] that the same kind of model, even without damping (dashpots), gives a fairly good representation of low Bond number sloshing. The model developed in Ref. [5], however, was limited to $h/d > 1$, no damping, zero degree contact angle, and a "free edge" or no contact angle hysteresis condition. Thus, in this report, the same model is extended to include linear viscous damping and any value of h/d. The zero degree contact angle and no hysteresis conditions are retained since these seem to be the most practical cases. A summary of the pertinent equations for the model is given in the Appendix.

For the proposed model, consisting of one mass, m_o, attached rigidly to the tank and one mass, m_1, attached to the tank through a spring (spring constant k_1) and dashpot (damping coefficient γ_s), the amplitude of the force response for simple harmonic excitation of frequency f is

$$F = 4\pi^2(m_o + m_1)x_o f^2 \left\{1 + \frac{m_1}{m_o + m_1}\left[\frac{(f/f_1)^2}{1 - (f/f_1)^2 + 2i\gamma_s(f/f_1)}\right]\right\} \tag{9}$$

where $i = \sqrt{-1}$. The parameters m_1, f_1, and k_1 (which are related through $2\pi f_1 = \sqrt{k_1/m_1}$) as calculated by the present theory are shown in Figs. 12, 13, and 14. All of the parameters are given as multiples of the corresponding high-g quantity calculated for the same R_o, h/d, g, and m_T ($m_T = m_o + m_1$ is the total mass of liquid contained in the tank); for reference, these high-g quantities are

$$\begin{aligned} f_1 &= \frac{1}{2\pi}\left\{1.841\,\frac{g}{R_o}\tanh 3.682\,\frac{h}{d}\right\}^{1/2} \\ m_1 &= 0.227 m_T\left(\frac{d}{h}\right)\tanh 3.682\,\frac{h}{d} \\ k_1 &= 0.337\left(\frac{g m_T}{h}\right)\left(\tanh 3.682\,\frac{h}{d}\right)^2 \end{aligned} \tag{10}$$

The low-g frequency, slosh mass, and frequency for $h/d = 1.0$ shown in the figures differ somewhat from the results presented in Technical Report No. 2 [5]; the difference is caused by retaining more terms here in the infinite series used to compute the model parameters.

By using the figures to calculate f_1, m_1, k_1, and $m_0 = m_T - m$, the force response for any N_{BO} and h/d can be determined. Comparisons of the force response predicted by the mechanical model to our experimental results are shown in Fig. 15 for four values of N_{BO} and four values of h/d; the value of γ_s used in Eq. (9) to compute the force corresponds to the experimental tests for the indicated x_o, R_o, h/d, and liquid. The comparison throughout the N_{BO} and h/d range is uniformly good, as can be seen. The darkened triangle (▼) along the frequency axis in each plot is the theoretical undamped natural frequency, f_1, whereas the peak in the resonance curve locates the damped resonant frequency; the difference between the two is entirely due to the damping.

Considering the good correlation between the frequency of the theoretical peak force and the experimental peak, it may be concluded that the curves in Fig. 12 adequately predict the low-g slosh frequency. Likewise, since the peak force for the theory and experiment are very close, the slosh mass m_1 is given adequately by Fig. 13.* Thus, the proposed mechanical model gives a good representation of the low-g sloshing dynamics.

*The peak force depends almost entirely on only m_1 and γ_s.

V. CONCLUSIONS

The experimental tests have verified that the use of small diameter tanks is adequate to simulate moderately low Bond number sloshing, including h/d variations and the effects of damping.

The smooth-wall damping coefficient was shown to increase as the Bond number decreased; for $N_{BO} > 10$, an adequate correlation of the damping coefficient is provided by either

$$\gamma_s = 0.83 N_{GA}^{-1/2} + 0.096 N_{BO}^{-1/2}$$

or

$$\gamma_s = 0.83 N_{GA}^{-1/2} \left(1 + 0.63 N_{BO}^{-1/2}\right)$$

The first equation predicts values of γ_s that are slightly more in agreement with experiment in the range $N_{BO} > 10$, but, the second, besides being in qualitative agreement with existing theories, seems to predict more reasonable values of γ_s for $N_{BO} < 10$. Neither correlation equation is correct for $N_{BO} = 0$.

The experiments, in conjunction with the theory, show that the low Bond number slosh mass, natural frequency, and spring constant all decrease more slowly as h/d decreases than do the corresponding high Bond number quantities. In other words, if the low Bond number parameters decreased at the same rate as did the high Bond number parameters, all of the frequency curves in Fig. 12, for example, would be parallel, and, in fact, all the curves would collapse onto the h/d = 1.0 curve. Since the smaller h/d curves are translated upward and moreover spread apart as N_{BO} decreases, it can be concluded that the frequency decreases less slowly with h/d than does tanh 3.682 h/d, which is the rate of decrease for large Bond number conditions.

Comparisons of the force response predicted by the theoretical model with the actual test values verify the mechanical model to about the same degree of confidence as similar models for high Bond number sloshing. The comparisons also show the importance of accounting for the damping in making natural frequency determinations; for example, with CCl_4 in a 0.383-in. diameter tank, the actual resonant frequency is about 9.7 cps (for h/d = 1.0), whereas the undamped natural frequency is 9.95 cps.

VI. LIST OF REFERENCES

1. Habip, L. M., "On the Mechanics of Liquids in Subgravity," Astronautica Acta, 11, No. 6, pp. 401-409 (1965).

2. Yeh, G. C. K., "Free and Forced Oscillations of a Liquid in an Axisymmetric Tank at Low-Gravity Environments," Trans. ASME, J. Applied Mech., 34, Series E, No. 1, pp. 23-28, March 1967.

3. Chu, W. H., "Low Gravity Liquid Sloshing in an Arbitrary Axisymmetric Tank Performing Translational Oscillations," Technical Report No. 4, Contract NAS8-20290, Southwest Research Institute, San Antonio, Texas, March 1967.

4. Hollister, M. P., Satterlee, H. M., and Cohan, H., "A Study of Liquid Propellant Behavior during Periods of Varying Accelerations," Final Report, Contract No. NAS9-5174, Lockheed Missiles and Space Company, Sunnyvale, California, June 1967.

5. Dodge, F. T., and Garza, L. R., "Experimental and Theoretical Studies of Liquid Sloshing at Simulated Low Gravities," Technical Report No. 2, Contract NAS8-20290, Southwest Research Institute, San Antonio, Texas, October 1966. (Also, Trans. ASME, J. Applied Mech., 34, Series E, No. 3, pp. 555-562, September 1967.)

6. Clark, L. V., and Stephens, D. G., "Simulation and Scaling of Low-Gravity Slosh Frequencies and Damping," AIAA Space Simulation Symposium Preprint, Philadelphia, Pennsylvania, September 1967.

7. Siegert, C. E., Petrash, D. A., and Otto, E. W., "Time Response of Liquid-Vapor Interface after Entering Weightlessness," NASA TN D-2458 (1964).

8. Salzman, J. A., Labus, T. L., and Masica, W. J., "An Experimental Investigation of the Frequency and Viscous Damping of Liquids during Weightlessness," NASA D-4132 (1967).

9. Abramson, H. N., Chu, W. H., and Kana, D. D., "Some Studies of Nonlinear Lateral Sloshing in Rigid Containers," Trans. ASME, J. Applied Mechanics, 33, Series E, No. 4, pp. 777-784, December 1966.

10. Stephens, D. G., Leonard, H. W., and Perry, T. W., "Investigation of the Damping of Liquids in Right-Circular Cylinders, Including the Effects of a Time Variant Liquid Depth," NASA TN D-1367 (1962).

11. Case, K. M., and Parkinson, W. C., "Damping of Surface Waves in an Incompressible Liquid," J. Fluid Mech., 2, pp. 172-184, March 1967.

12. Keulegan, G. H., "Energy Dissipation in Standing Waves in Rectangular Basins," J. Fluid Mech., 6, pp. 33-50, July 1959.

13. Miles, J. W., "Surface Wave Damping in Closed Basins," Proc. Royal Society (London), 297 A, No. 1451, pp. 459-475, March 1967.

APPENDIX A

THEORY - MECHANICAL MODEL

To derive the velocity potential for liquids of finite depth, it is only necessary to replace $\exp(\lambda_n Z)$ in Eq. (19) of Ref. [5] by $\cosh \lambda_n Z + \tanh \lambda_n h/R_o \sinh \lambda_n Z$. The Fourier-Bessel expansion coefficients, $C1_{nm}$, $C2_{nm}$, and $C3_{nm}$ [Eqs. (21) of [5]*], then become

$$C1_{nm} = \frac{2\lambda_n^2}{(\lambda_n^2 - 1)[J_1(\lambda_n)]^2} \int_0^1 \Big\{ -\lambda_m J_1(\lambda_m R)[\sinh \lambda_m F + \tanh \lambda_m \frac{h}{R_o} \cosh \lambda_m F] + \frac{3}{2} \beta R^2 (1 - R^3)^{-1/2} J_1'(\lambda_m R)[\cosh \lambda_m F + \tanh \lambda_m \frac{h}{R_o} \sinh \lambda_m F] \Big\} R J_1(\lambda_n R)\, dR$$

$$C2_{nm} = \frac{2\lambda_n^2}{(\lambda_n^2 - 1)[J_1(\lambda_n)]^2} \int_0^1 [\cosh \lambda_m F + \tanh \lambda_m \frac{h}{R_o} \sinh \lambda_m F] R J_1(\lambda_m R) J_1(\lambda_n R)\, dR$$

$$C3_{nm} = \frac{2\lambda_n^2}{(\lambda_n^2 - 1)[J_1(\lambda_n)]^2} \int_0^1 \frac{R J_1(\lambda_n R)}{\left(1 - R^3 + \frac{9}{4}\beta^2 R^4\right) N_{BO}} \Big\{ J_1(\lambda_m R) \times \left[\lambda_n^2 (1 - R^3)^{3/2} + \frac{9}{4} \beta^2 R^2 (1 - R^3)^{1/2} \right] + \frac{27\beta^2 R^3 (1 - R^3)^2 (1 - 0.25R^3) J_1'(\lambda_m R)}{2\left(1 - R^3 + \frac{9}{4}\beta^2 R^4\right)} \Big\}\, dR$$

By using these equations to calculate $C1_{nm}$, $C2_{nm}$, and $C3_{nm}$ numerically, all of the remaining quantities of interest can be determined as described in Ref. [5]. The results for f_1, m_1, and k_1 shown in Figs. 12, 13, and 14 were computed using the first five terms in the infinite series defining them; this was more than adequate to insure convergence as long as $N_{BO} > 10$.

---

*The misprints in the definitions of $C1_{nm}$, $C2_{nm}$, $C3_{nm}$ of Ref. [5] have been corrected here.

APPENDIX B

ILLUSTRATIONS

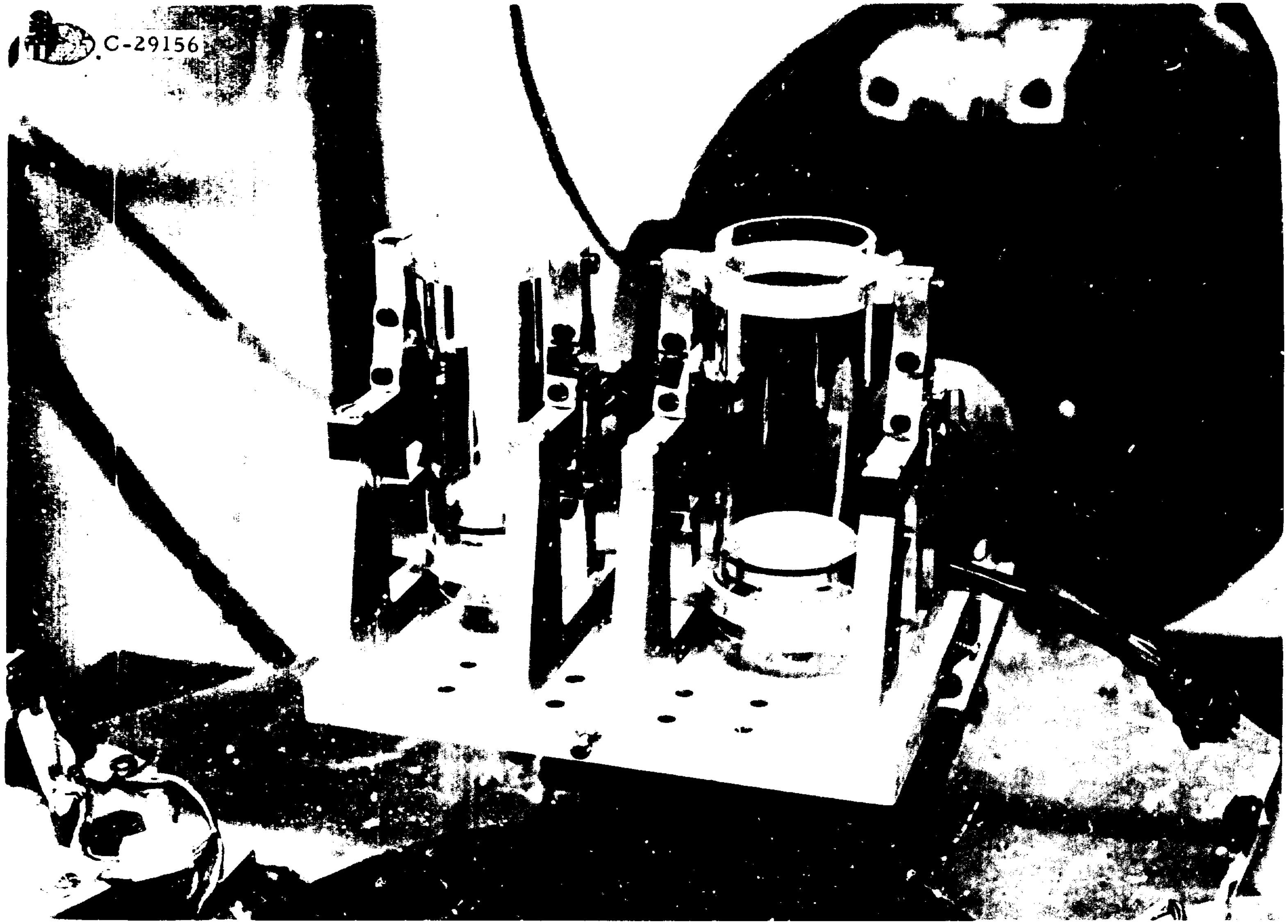

Figure 1. Dynamometer Package On Shake Table

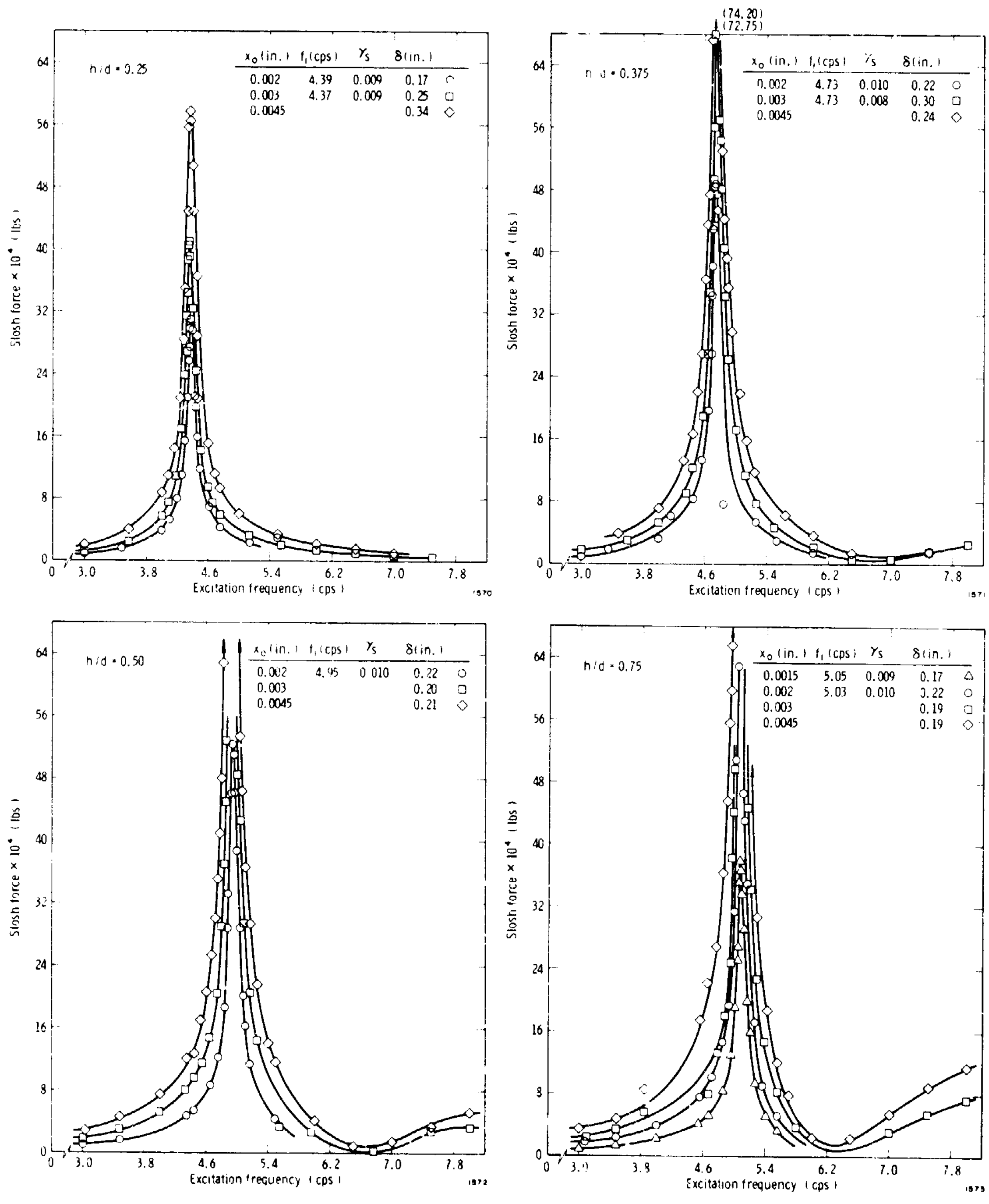

Figure 2. Response Curves For CCl_4 In 1.36" Dia. Tank, N_{BO} = 175

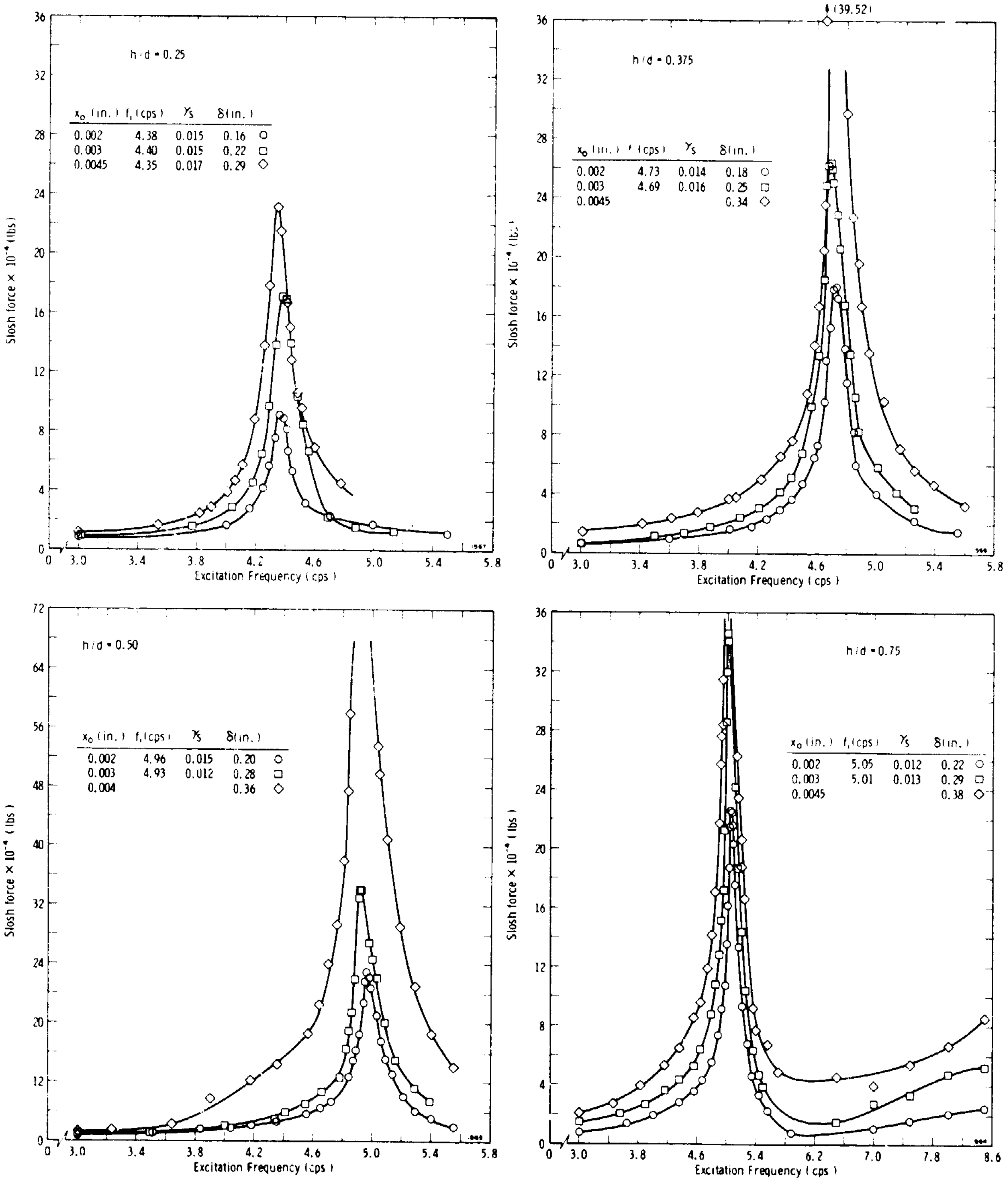

Figure 3. Response Curves For Methanol In 1.36" Dia. Tank, N_{BO} = 100

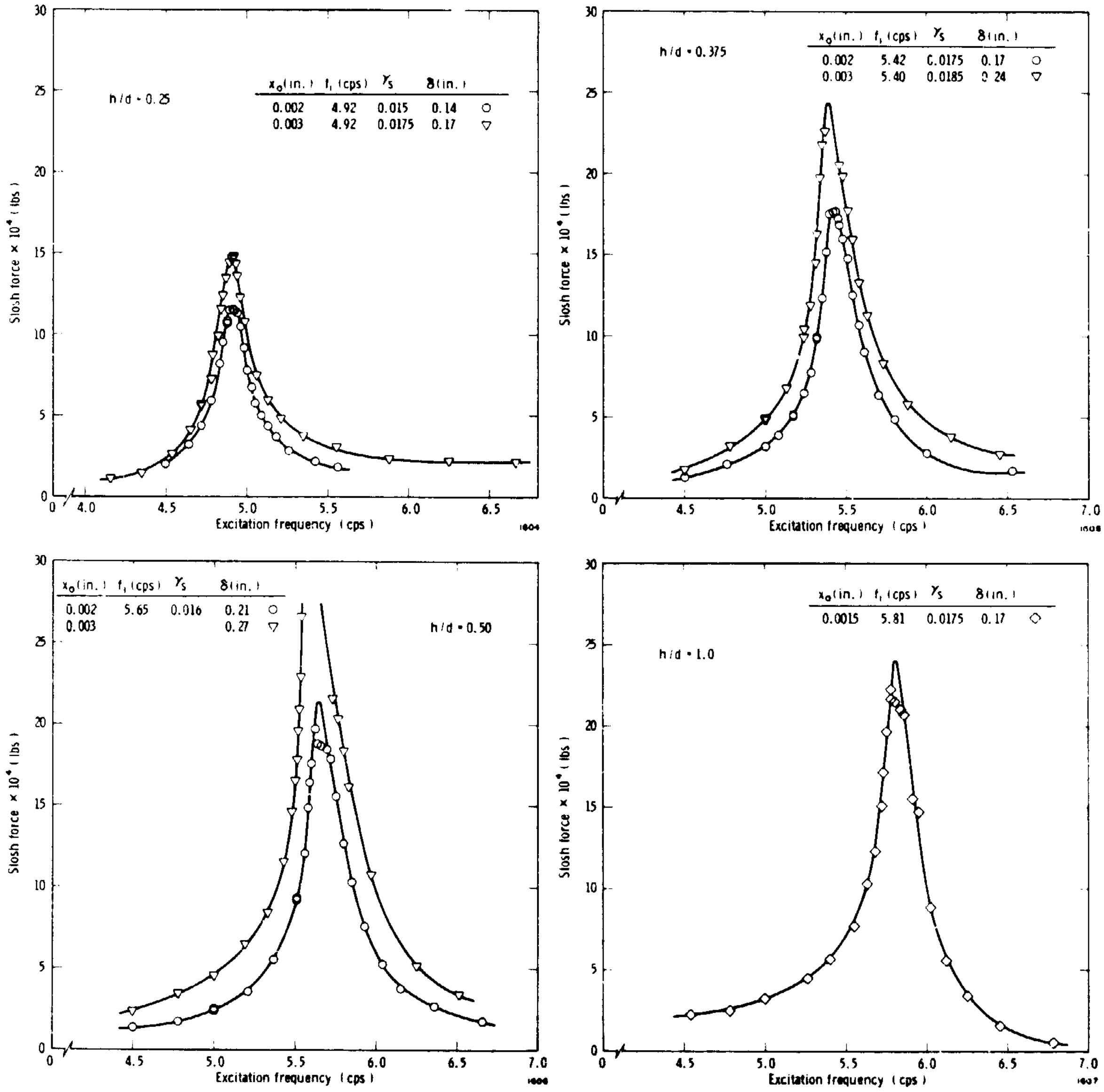

Figure 4. Response Curves For CCl_4 In 1.04" Dia. Tank, N_{BO} = 100

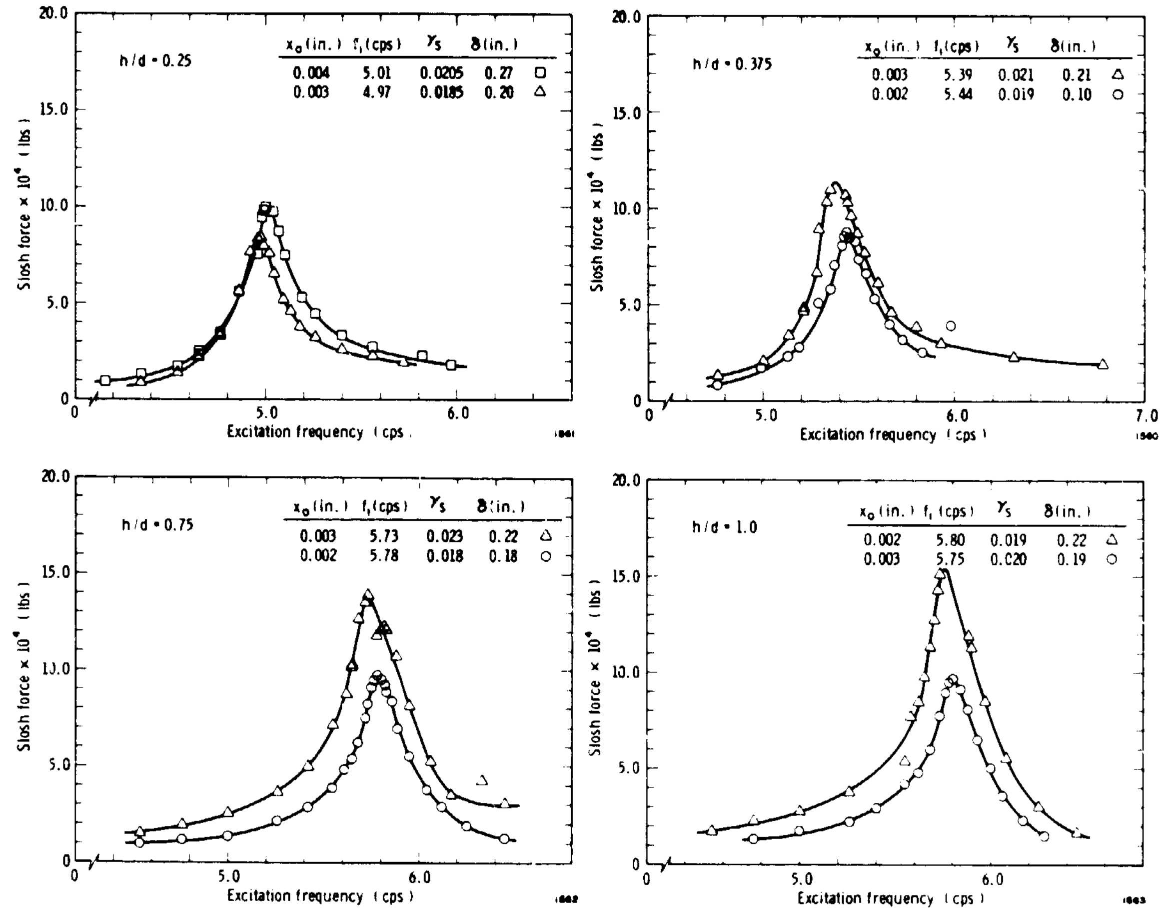

Figure 5. Response Curves For Methanol In 1.04" Dia. Tank, N_{BO} = 60

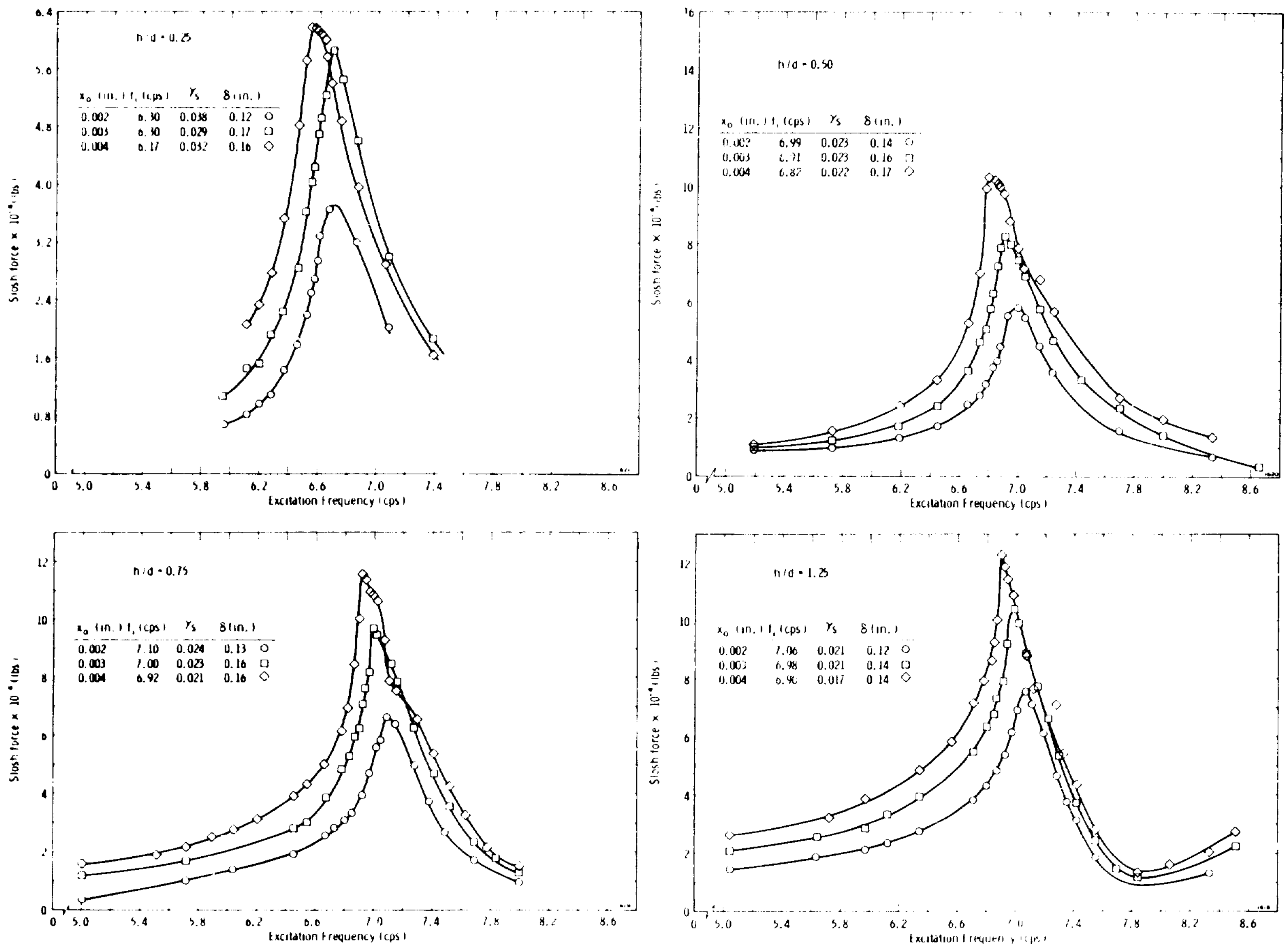

Figure 6. Response Curves For $CC\ell_4$ In 0.688" Dia. Tank, N_{BO} = 45

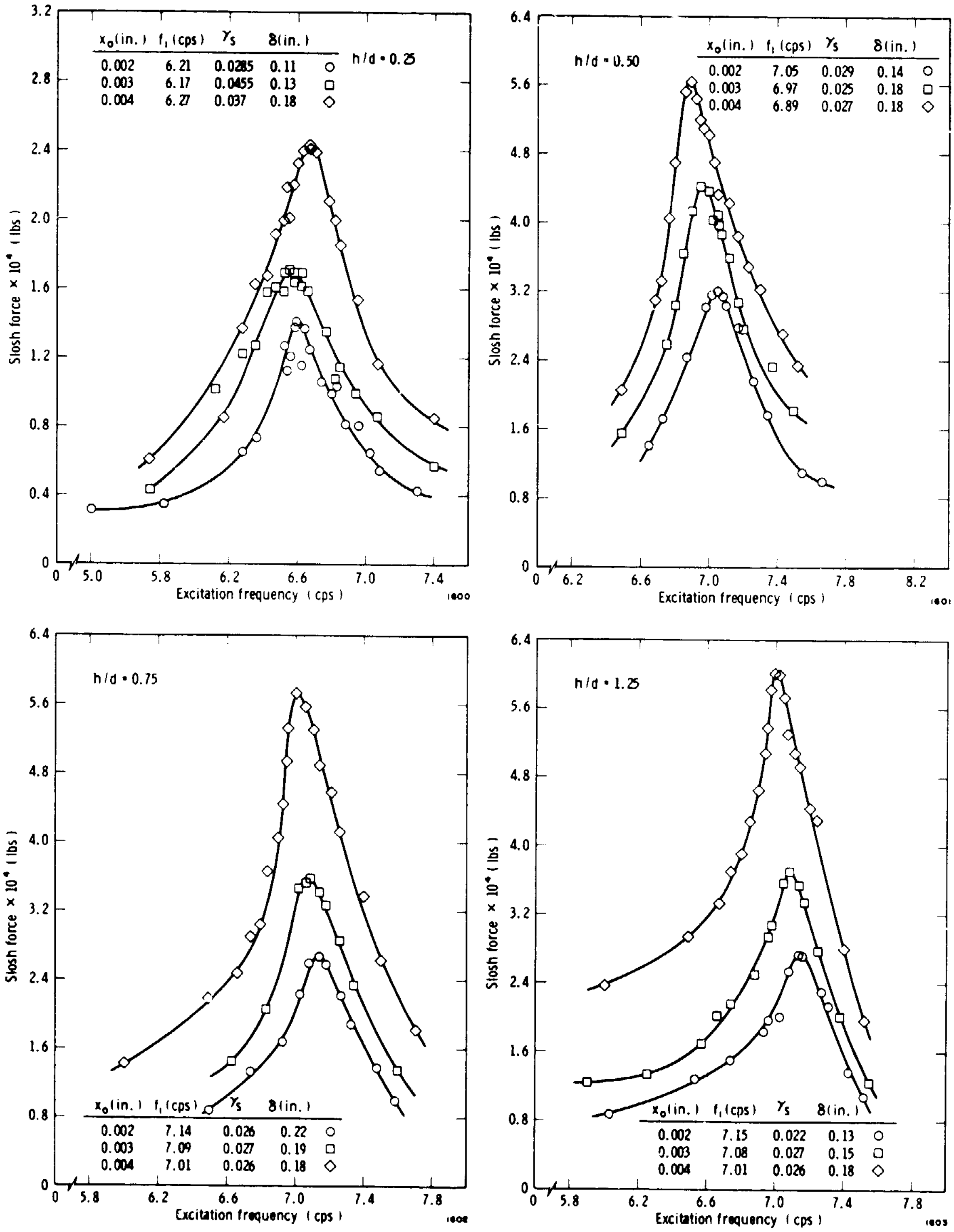

Figure 7. Response Curves For Methanol In 0.688" Dia. Tank, N_{BO} = 26

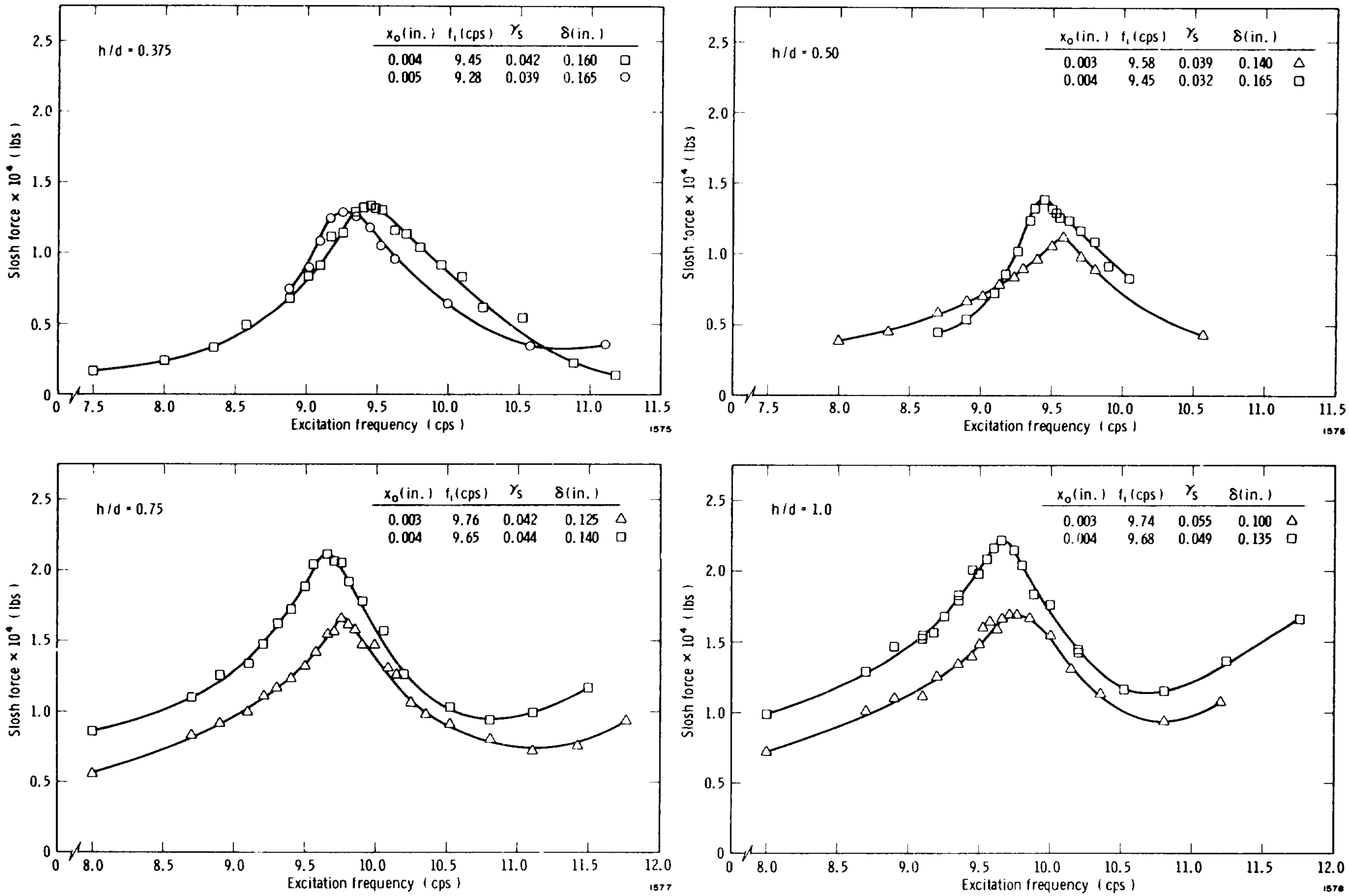

Figure 8. Response Curves For $CC\ell_4$ In 0.383" Dia. Tank, N_{BO} = 14

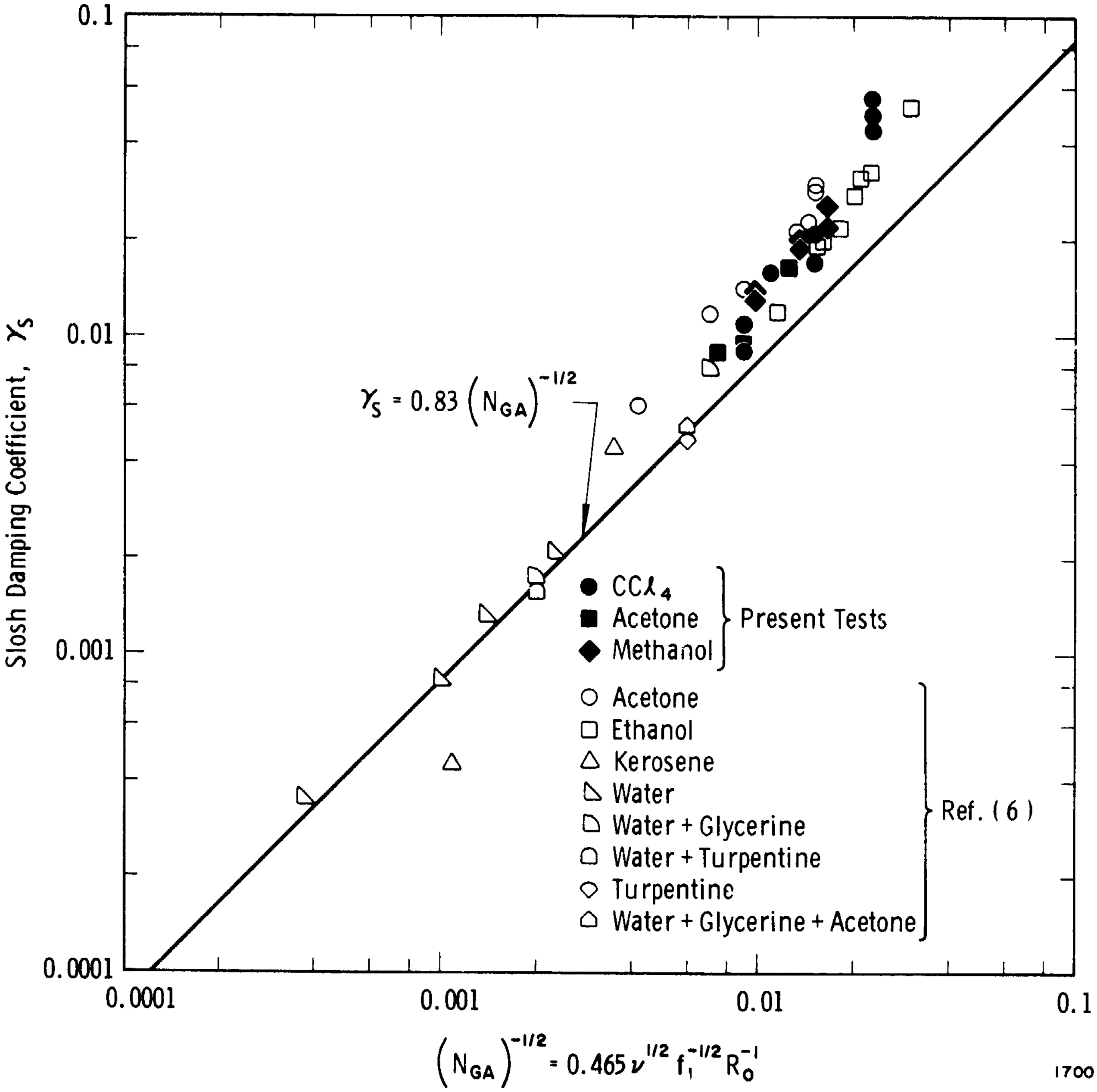

Figure 9. Variation Of Smooth Wall Damping Coefficient With Galileo Number

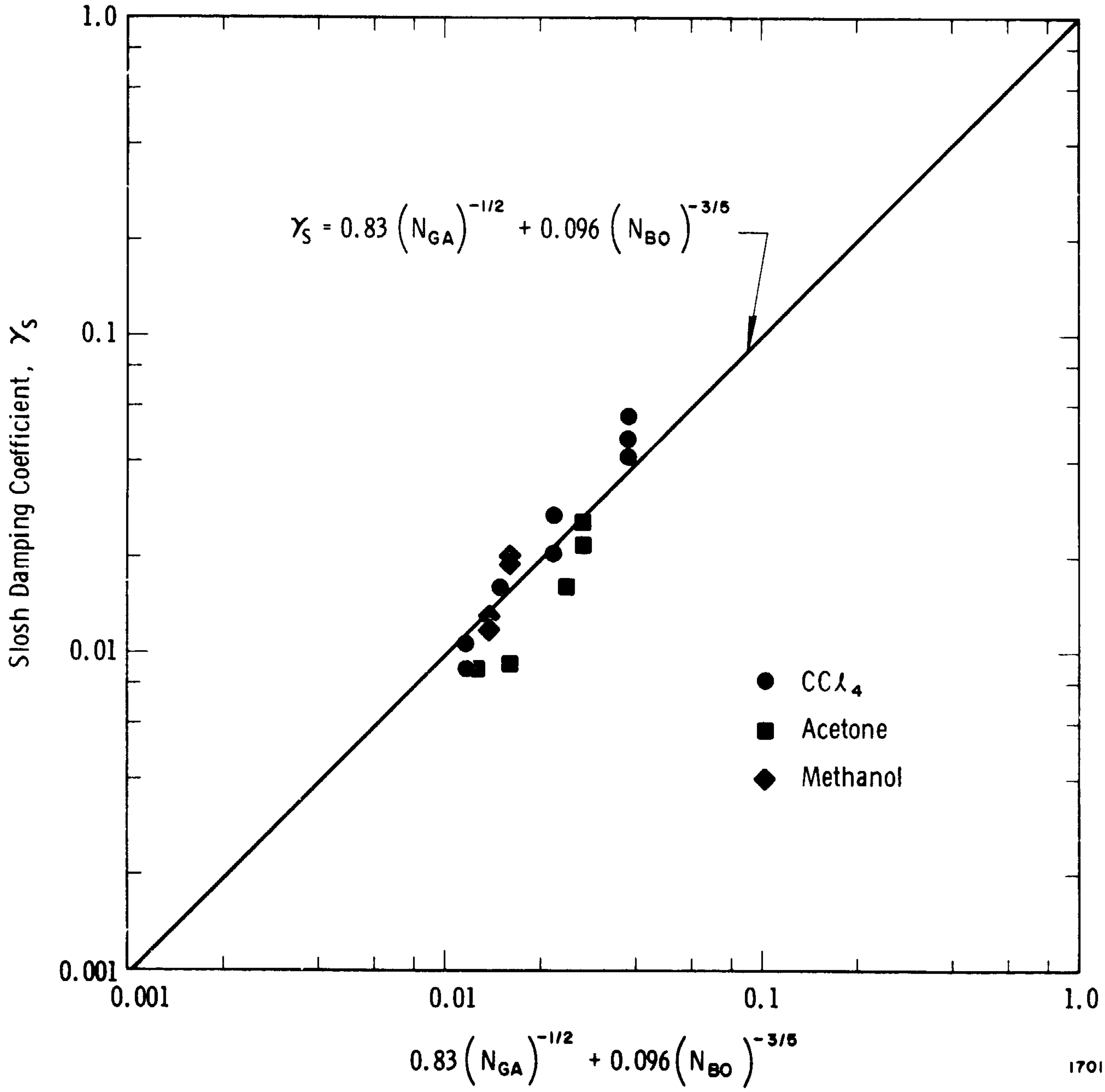

Figure 10. Variation Of γ_S With Correlation Equation Of Clark And Stephens [6]

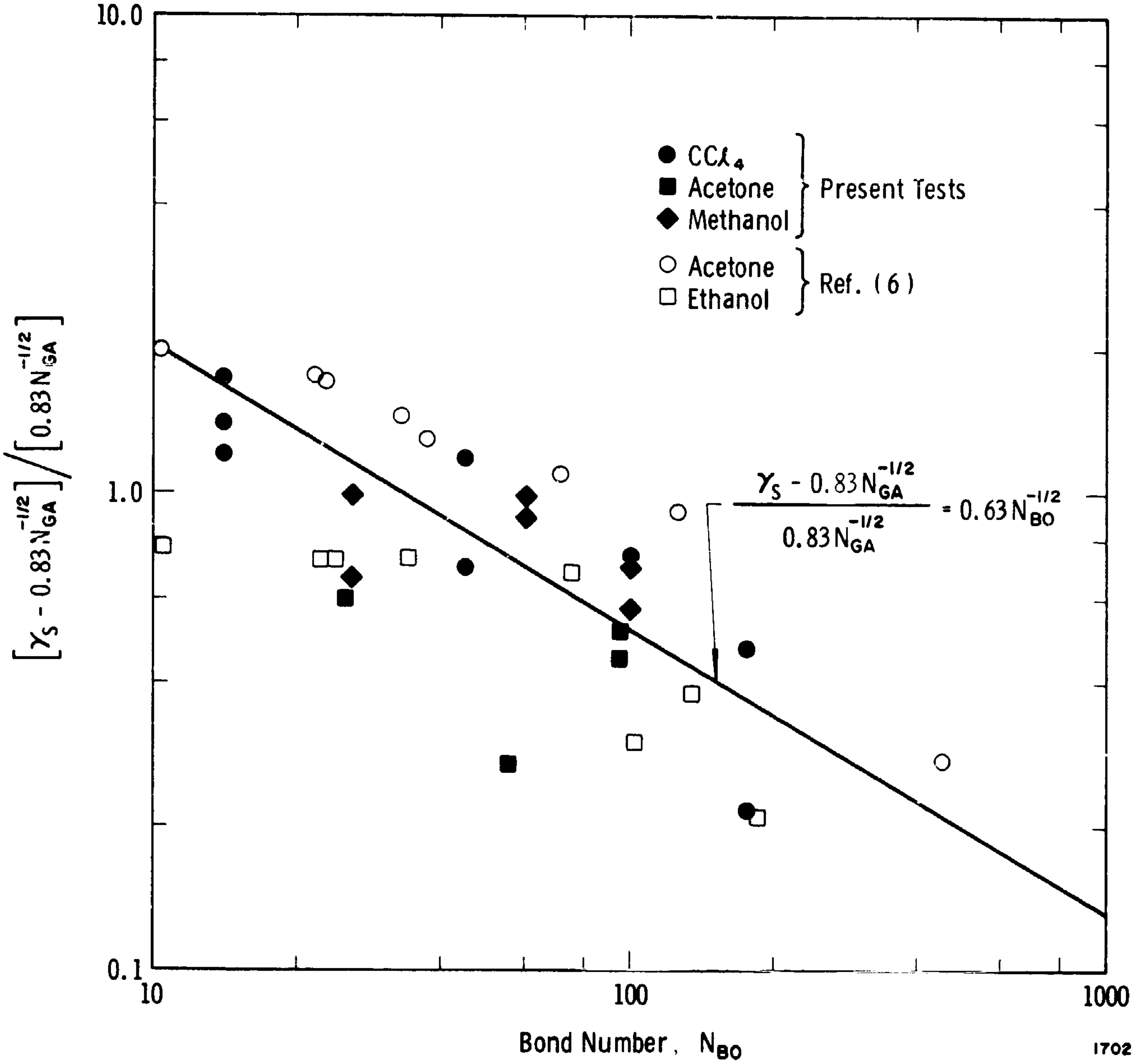

Figure 11. Variation Of Incremental Damping Factor With Bond Number

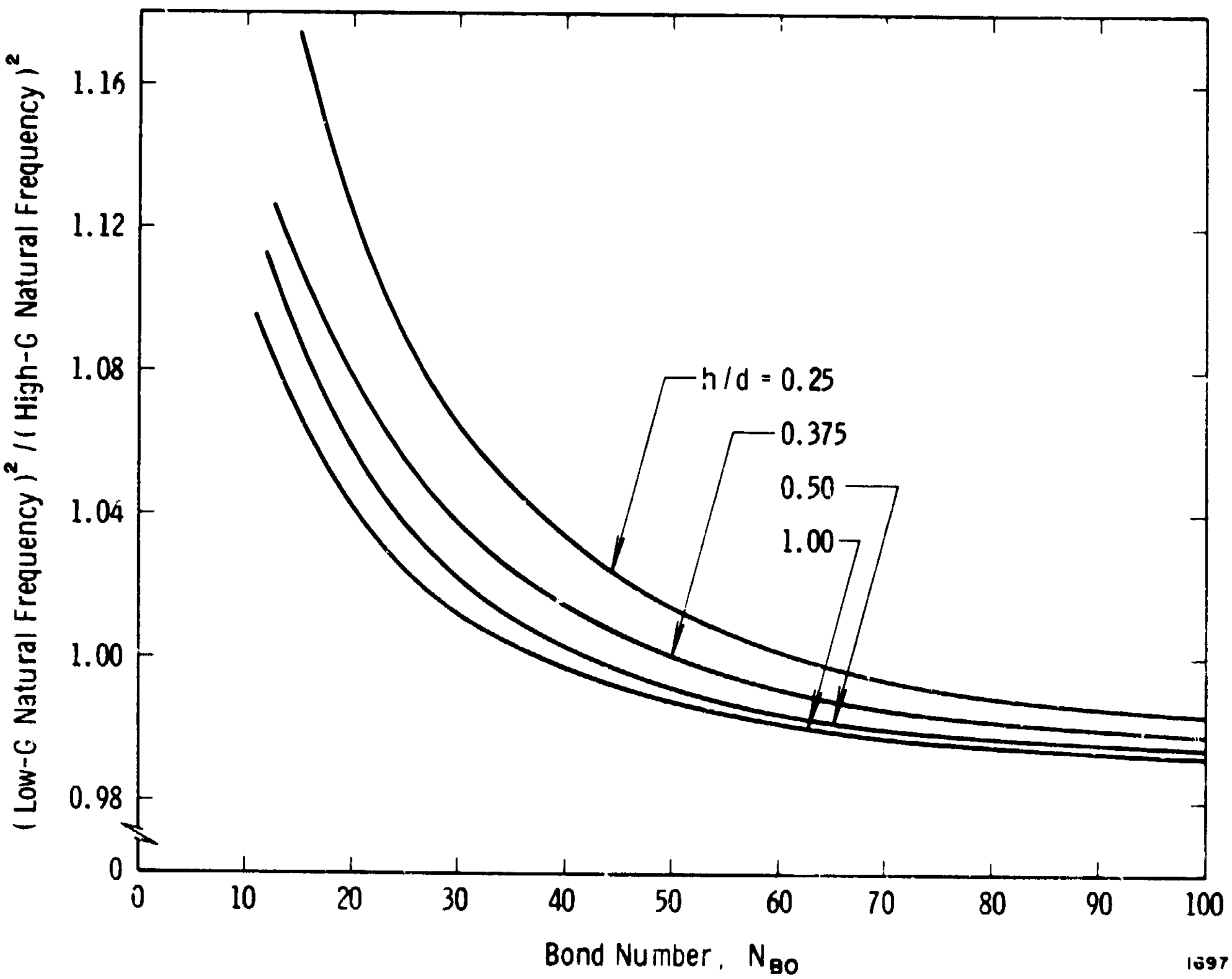

Figure 12. Variation Of Slosh Natural Frequency With Bond Number

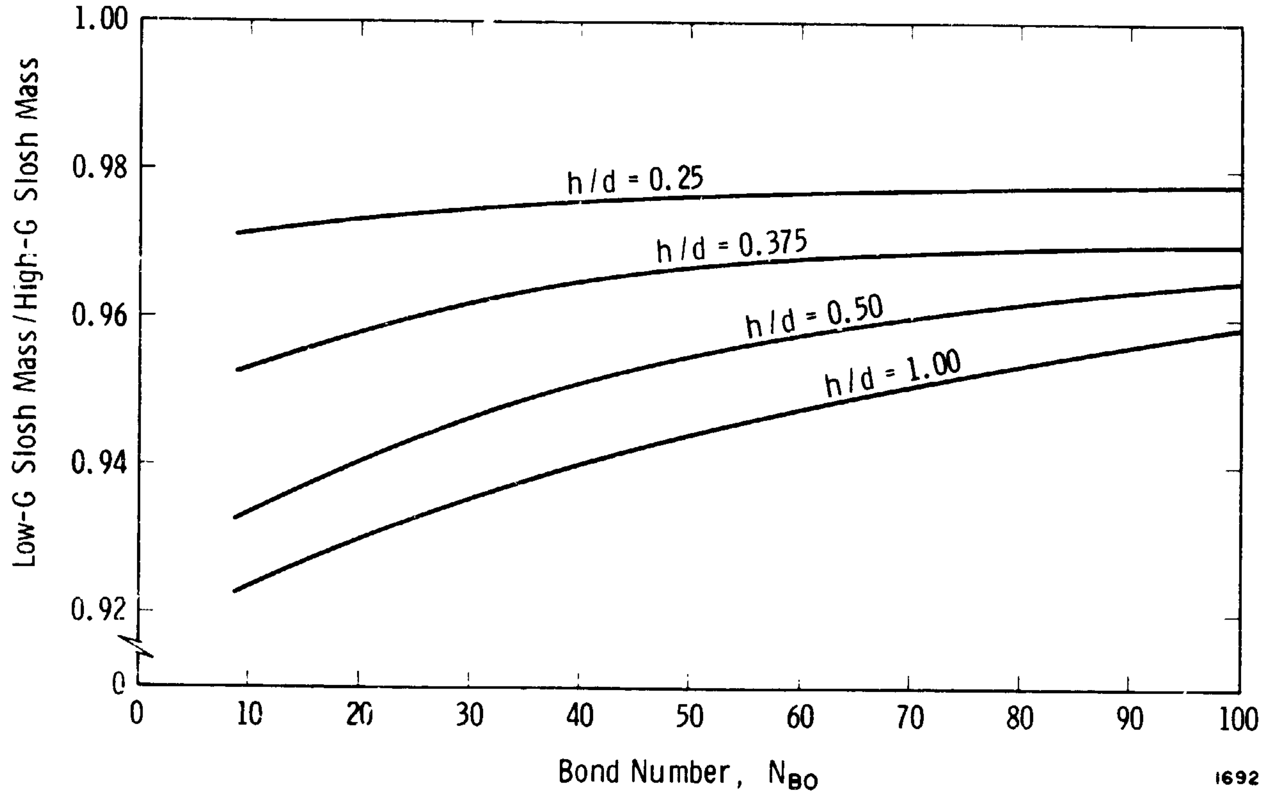

Figure 13. Variation Of Slosh Mass With Bond Number

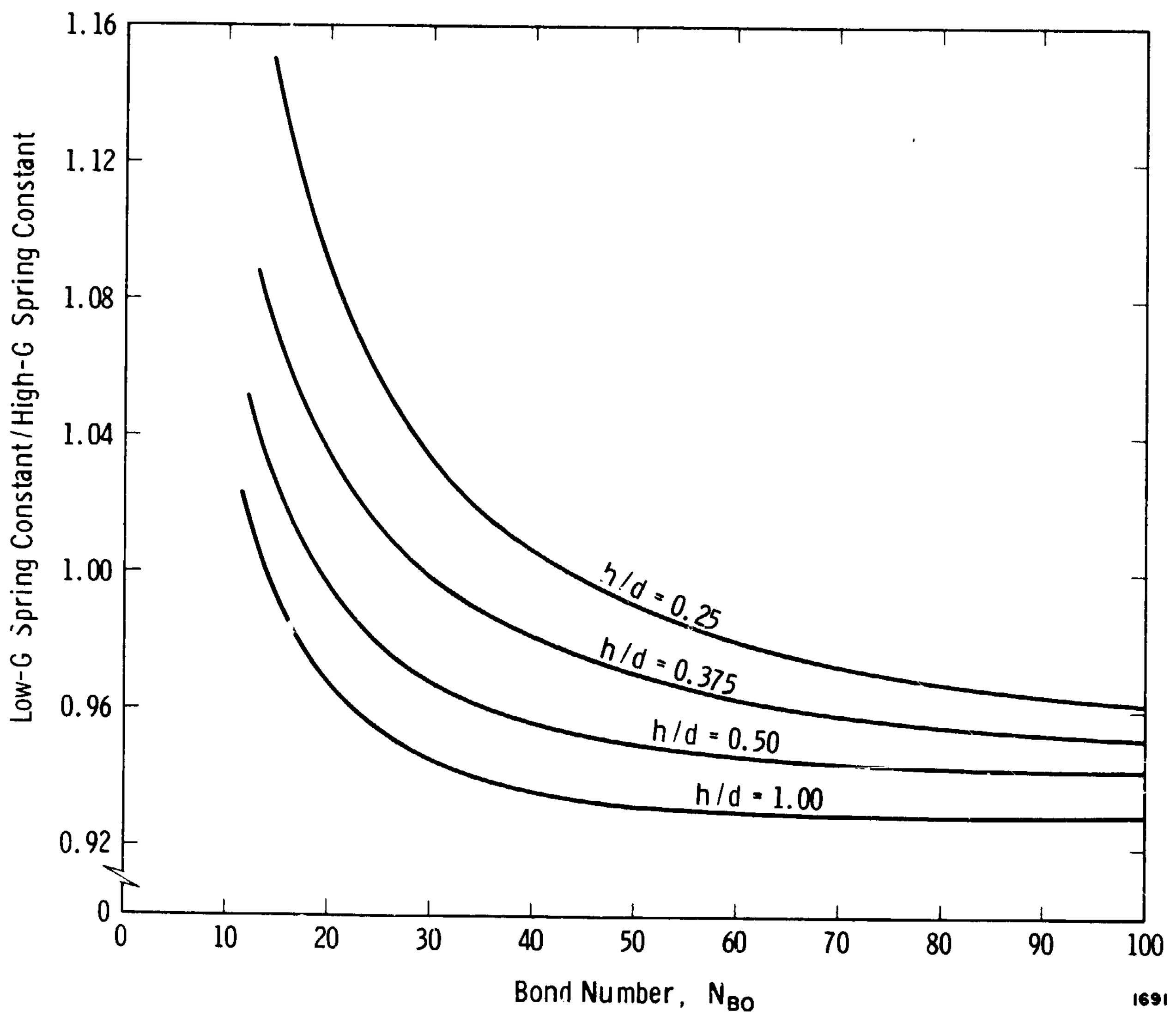

Figure 14. Variation Of Spring Constant With Bond Number

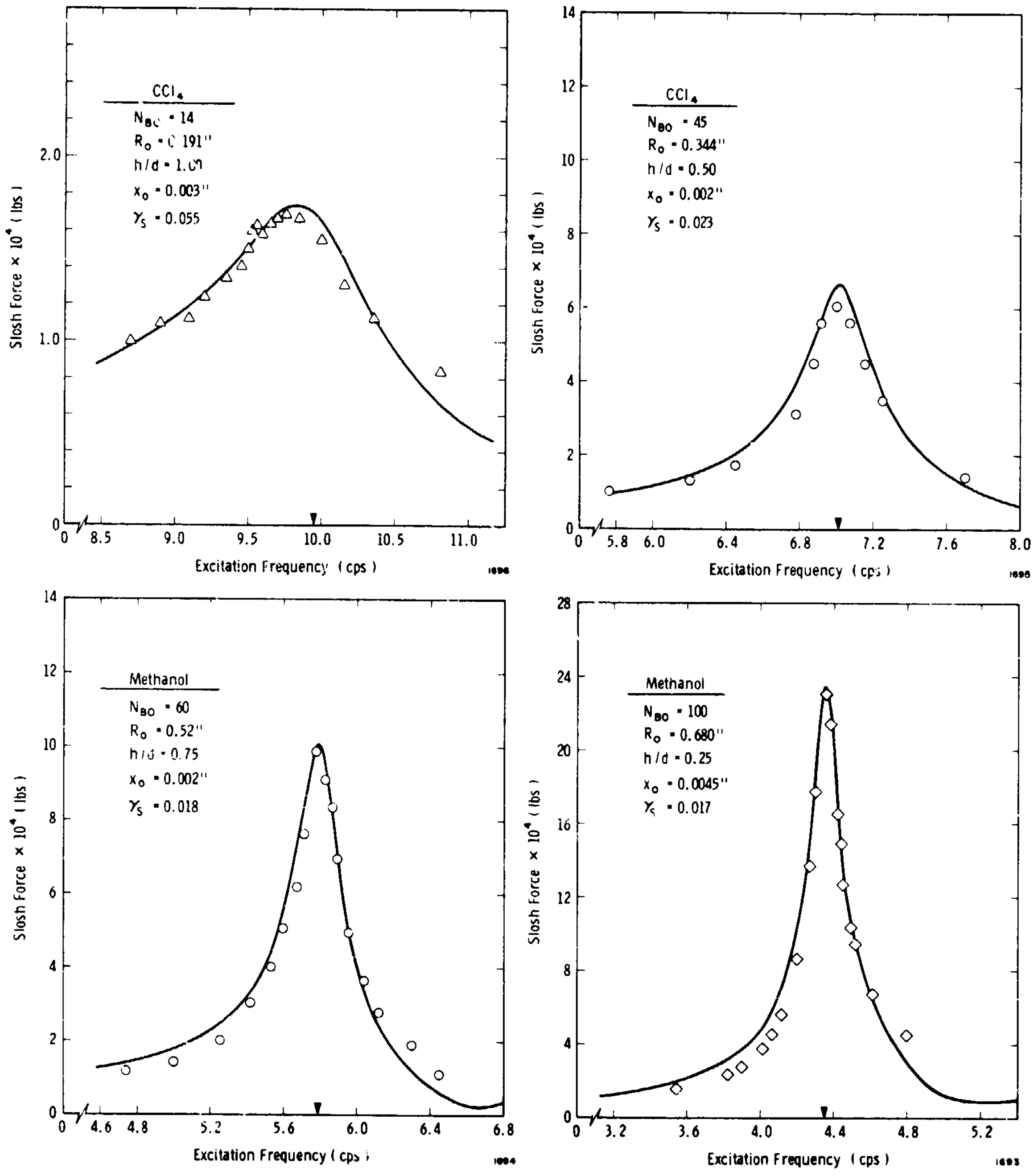

Figure 15. Comparison Of Theoretical And Experimental Force - Response Curves

ERRATA

"Simulated Low-Gravity Sloshing in Cylindrical Tanks Including Effects of Damping and Small Liquid Depth," Technical Report No. 5, Contract NAS8-20290

page 8, 2nd line above Eq. (8): this line should read "...to Eq. (7) was obtained with A = 8.20 and n = -3/5; the proposed correla-...."

page 8, Eq. (8): should read " $\gamma_s = 0.83 N_{GA}^{-1/2}(1 + 8.20 N_{BO}^{-3/5})$ "

page 9, line 2: the value of N_{BO} should be 4.0 and not 0.03

page 9, lines 5 and 6: delete and replace by "...of Ref. [7], but for $N_{BO} = 4.0$, Eq. (2) predicts that $\gamma_s = 0.83 N_{GA}^{-1/2} + 0.042$, which is about of the correct numerical magnitude. Note, also, that γ_s varies with N_{BO} in the same way in both Eq. (2) and Eq. (8)."

page 12, 2nd equation after line 6: should read " $\gamma_s = 0.83 N_{GA}^{-1/2} (1 + 8.20 N_{BO}^{-3/5})$ "

page 27, Figure 11: the equation given in the figure should be

$$"\frac{\gamma_s - 0.83 N_{GA}^{-1/2}}{0.83 N_{GA}^{-1/2}} = 8.20 N_{BO}^{-3/5}"$$

END

DATE

FILMED

MAR 4 1968